THE JOURNAL OF COMPARATIVE NEUROLOGY 255:560–570 (1987)

Hair Cell Innervation by Spiral Ganglion Neurons in the Mouse

A.M. BERGLUND AND D.K. RYUGO
Department of Anatomy and Cellular Biology, Harvard Medical School, Boston, Massachusetts 02115 and Eaton-Peabody Laboratory, Massachusetts Eye and Ear Infirmary, Boston, Massachusetts 02114

ABSTRACT

Horseradish peroxidase (HRP) was injected extracellularly into the auditory nerve of adult mice so that the enzyme could infuse individual spiral ganglion neurons. Forty-two well-stained neurons were reconstructed through serial sections from their cell bodies to peripheral terminations in the organ of Corti with the aid of a light microscope and drawing tube. No neuron was observed to innervate both inner and outer hair cells (IHCs and OHCs). Previous observations from neonatal mammals that reported that IHCs and OHCs were innervated by the same neuron are thus presumed to describe a transient developmental phenomenon.

Two populations of spiral ganglion neurons were determined on the basis of the differences in receptor innervation. The type I neurons innervated exclusively IHCs by way of thick (1–2 μm) radial fibers, whereas the type II neurons innervated only OHCs by way of thin ($\sim$0.5 μm) outer spiral fibers. Certain features of the peripheral process in the vicinity of the cell body were highly correlated with fiber type. This pattern of separate innervation of IHCs and OHCs by type I and type II neurons, respectively, may represent the general plan of afferent organization for the adult mammalian cochlea.

Key words: auditory system, hearing, primary afferents, receptors, type I spiral ganglion cells, type II spiral ganglion cells.

In the mammalian cochlea, inner hair cells (IHCs) and outer hair cells (OHCs) are the two types of sensory receptors (von Ebner, '03; Held, '26). These receptors are involved in the transduction of acoustic energy into spike discharges of cochlear neurons (Davis '58; Weiss, '84). The output of the receptors is conveyed as input to the brain by way of these primary neurons, the cell bodies of which reside in the spiral ganglion and the central axons of which form the auditory nerve. There are at least two types of cell bodies in the spiral ganglion (Münzer, '31; Rasmussen, '43). Knowledge of how receptors and ganglion cells are connected is basic to understanding the nature of the signals delivered to the central nervous system.

In adult cats, there is a segregation of afferents from the two types of hair cells (Spoendlin, '73; Kiang et al., '82; Ginzburg and Morest, '83). A group of large, generally bipolar ganglion cells innervate IHCs by means of thick radial fibers; a group of smaller, pseudomonopolar ganglion cells innervate OHCs by means of thin outer spiral fibers. No individual ganglion cell was observed to contact both types of receptors. This morphological arrangement appears to provide two separate afferent channels for the auditory system of cats. In contrast, Golgi studies in young rodents (mice, rats, and guines pigs) portrayed three patterns of afferent cochlear innervation: There were radial fibers, outer spiral fibers, and fibers that distributed terminals to both IHCs and OHCs (von Ebner, '03; Lorente de Nó, '37; Polyak et al., '46; Perkins and Morest, '75). We questioned whether the observed innervation differences could be attributable to transient developmental characteristics resulting from differences in the relative age of the specimens examined or to fundamental species differences in the way in which the auditory nerve is connected to the peripheral receptors. The pattern of receptor innervation by primary afferent neurons has obvious implications concerning neural mechanisms involved with the initial processing of acoustic information.

The present study was undertaken to examine hair cell innervation by spiral ganglion neurons in adult mice and to test the generality of the concept that two types of spiral ganglion cells separately innervate the two types of acoustic receptors. In view of the widely different ecological niches occupied by mammals, innervation patterns of a general

Accepted July 8, 1986.

nature must be distiguished from those representing more specialized, species-specific requirements. HRP was injected extracellularly into the auditory nerve, and after histological processing, individual neurons were diffusely and darkly stained from the injection site to their peripheral terminations in the cochlea. Single neurons were reconstructed through serial sections revealing two distinct afferent pathways in the peripheral auditory system of the mouse.

MATERIALS AND METHODS

The data here were obtained from male albino mice, aged 6–10 weeks (CD-1, Charles River Laboratories, Wilmington, MA). Although there have been recent objections to the use of albinos for auditory research (e.g., Bock and Steel, '84), albino mice have proven quite useful for many research questions where albinism *per se* did not affect the results (e.g. Henry, '83; Ryugo and Willard, '85). In addition, a pilot study using silver stains revealed degenerative changes in the auditory nerves of 60-day-old pigmented (C57/B) but not albino (CD-1) mice (unpublished observations). Finally, we found that the surgical exposure of the auditory nerve in albino mice resulted in far fewer fatalities due to excessive bleeding than in pigmented mice.

Surgery and injection parameters

The mice were anesthetized with Avertin (5 g of 2,2,2-tribromoethanol dissolved in 3 ml of amylene hydrate and diluted 1:20 in physiological saline) at a dose of 0.2 cc per 10 g body weight. By using a dorsal surgical approach, the lateral cerebellum and paraflocculus were aspirated in order to see the cochlear nucleus, and then the cochlear nucleus was retracted medially in order to expose the auditory nerve. A silicone-coated glass micropipette (I.D.: 30–40 μm) filled with HRP (Sigma type VI, 36% w/v) in 0.1 M Tris buffer (pH 8.6) was lowered into the nerve under direct visual control. The injections (two to four per nerve) were accomplished by applying 2 μA of positive current (continuous or 50% duty cycle) for 5-10 minutes.

Histological processing

Each animal was given a lethal dose of Avertin 2–24 hours after the injection of HRP. Intracardiac and subsequent labyrinthine perfusions were conducted with 1.25% paraformaldehyde and 2.5% glutaraldehyde in 0.1 M phosphate buffer. The tissue was postfixed for 24 hours, after which the cochlea was dissected, decalcified in 0.1 M EDTA (pH 7.3), embedded in gelatin-albumin (Frank et al., '80), and sectioned perpendicular to the modiolus (80-μm thickness) on a Vibratome. Free-floating cochlear sections were treated with diaminobenzidine (e.g., Liberman and Oliver, '84), mounted in serial order on "subbed" slides, dehydrated in ethanol, and coverslipped with Permount.

Data analysis

Cells varied greatly in the amount of intracellular HRP reaction product. We focused our attention on diffusely and darkly stained spiral ganglion cells. Such cellular staining resembled Golgi-like impregnations and allowed us to trace certain individual neurons unambiguously from cell body to termination against hair cells. These spiral ganglion cells were then reconstructed from serial sections with a light microscope and drawing tube (magnification = x1,250), enlarged to a total magnification of x3,380, and analyzed quantitatively with the aid of a computerized planimeter. Means, standard errors of the mean, and Smirnov's (nonparametric) P values (two-tailed test) are provided where appropriate. The following criteria were applied to delineate the morphological features that were measured in this study:

Cell body silhouette area. The cell body was operationally separated from the processes by drawing a line that connected the "subjective" middle of opposing concavities (Fig. 1, top). The shaded area represents the cell body silhouette.

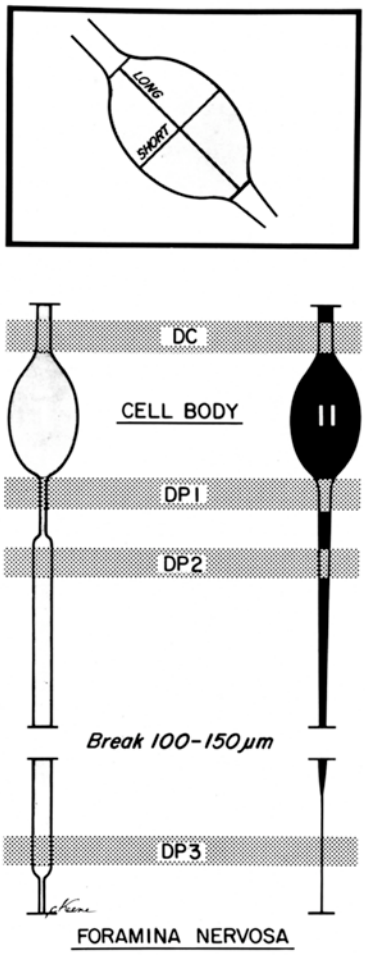

Fig. 1. Top: Schematic diagram indicating how the spiral ganglion cell body (shaded area) was separated from the processes for measurement purposes. Boundary lines were drawn through the approximate middle of each concavity flanking the central and peripheral processes. The long axis of each cell was represented by a line drawn through the opposing process. The short axis is a line perpendicular to the first, and is indicative of the maximum width of the cell body. Bottom: Diagram indicating where standardized segments of individual fibers were measured. The shaded areas represent 10-μm process segments used for determining average process diameters, DC, DP-1, DP-2, and DP-3. DC; explanation given in text.

Long and short somatic axes. The long axis was drawn to bisect the opposing processes; the short axis was represented by the maximum width of the cell body perpendicular to the long axis. The long/short axis ratio was used as a roundness coefficient for the cell body (Kiang et al., '84).

Relative position in ganglion. The shortest distance from the geometric center of each labelled cell body to the peripheral boundary of the ganglion was measured. The outer periphery of the intraganglionic spiral bundle was used to mark the ganglion boundary. For each reconstructed neuron, this distance represented its radial position within the ganglion.

Fiber diameter at selected sites. The average process diameters for selected 10-μm segments were determined for each reconstructed fiber (Fig. 1, bottom). The diameters of the central process (DC) and peripheral process (DP-1) were measured immediately adjacent to the cell body. The peripheral process of each radial fiber was extremely thin as it left the cell body but within 25 μm it abruptly thickened; this initial thickened segment was termed DP-2. The peripheral process of outer spiral fibers did not exhibit any thickening, so in order to standardize the location of DP-2 for both fiber types, outer spiral fiber measurements were taken 25 μm from the cell body. A final diameter measurement, DP-3, was taken at the level of the foramina nervosa, just before the afferent fibers enter the organ of Corti. Average process diameter was calculated by dividing the silhouette area of the segment by its length.

Terminal silhouette area. The termination of each radial fiber was characterized by a swelling. The border between radial fiber and terminal swelling was operationally defined by paired concavities that initiate the swelling. A connecting line was drawn through the concavities, isolating each swelling and enabling us to determine silhouette area. Because the terminal swellings of outer spiral fibers were smaller and more faintly labelled, we were not confident of their measurements and so have not included them.

Untraced neurons. A second set of data was collected from a sample of cell bodies and their immediately adjacent fiber segments (n=100) and outer spiral fibers (n=6) not traced throughout their entire peripheral extension. The regularity of the peripheral process characteristics of traced type II neurons permitted us to identify the other six untraced outer spiral fibers by applying the following criteria: (1) each outer spiral fiber crossed the tunnel of Corti near the floor; (2) once the outer spiral fibers entered the OHC region, each spiralled in a basal direction; and (3) each outer spiral fiber spiralled for at least 100 μm before emitting short terminal branches. These data were used to supplement descriptions of reconstructed neurons.

Nomenclature. There are a few terms that require definition. A fiber is said to "bifurcate" when daughter branches are of approximately equal caliber and length. "Terminal branches" are thin, short, and generally have a distinct swelling at their tips. "Spiral length" refers to the portion of an outer spiral fiber that travels immediately beneath the outer hair cells prior to emitting terminal branches. "Terminal spiral length" refers to the outer spiral fiber segment over which terminal branches are emitted.

RESULTS

This light microscopic report is based primarily on 42 completely reconstructed cells from eight adult mice. The HRP reaction product clearly revealed silhouettes of well-stained neurons but obscured intracellular features of the cell body (such as Nissl bodies and nucleus). Most descriptions pertain to the middle third of the cochlear spiral. The peripheral process of each ganglion cell was traced to either IHCs or OHCs and no cell was observed to innervate both types of receptors. Type I (n=29) neurons contacted IHCs by way of radial fibers and type II neurons (n=13) contacted OHCs by way of outer spiral fibers (Fig. 2). Morphological features of the two kinds of spiral ganglion neurons are summarized in Table 1.

Innervation characteristics

The peripheral process of each type I neuron always exhibited a thin ($\sim$0.5 μm) segment in the vicinity of the cell body. This segment abruptly thickened (1–2 μm) within 25 μm of the cell body and remained relatively constant in diameter (except for occasional constrictions as the fiber traveled radially though the osseous spiral lamina. The constrictions have the appearance of nodes of Ranvier. Each radial fiber again became thin as it passed through a foramen nervosum, entered the organ of Corti, and approached an IHC. The terminal portion of the radial fiber was a swelling of variable size and shape that abutted in most cases the lateral side or base of a single IHC (Fig. 3). On two occasions, the terminal portion of the radial fiber bifurcated; one radial fiber contacted two adjacent IHCs whereas the other supplied two endings against a single IHC. Both of these branched radial fibers were located in the basal region of the cochlear duct of the same animal.

Each type II neuron sent a thin peripheral process radially across the osseous spiral lamina. The outer spiral fiber exhibited its maximum diameter in the vicinity of the cell body and gradually tapered until it reached a relatively constant average diameter (0.4 μm) at the level of the organ of Corti. Outer spiral fibers coursed beneath the IHCs, but no branching was visible. Swellings were occasionally present along outer spiral fibers in this region but never abutted IHCs. After passing under the row of IHCs, each outer spiral fiber crossed the tunnel of Corti near its floor, turned basally, and then spiralled along the base of the OHCs prior to emitting three to ten branches (mean: 6.2 $\pm$ 0.6). The trajectory of outer spiral fibers was relatively constant, but their terminal regions were more variable. The terminal branches of one outer spiral fiber contacted adjacent OHCs, whereas a different outer spiral fiber contacted alternate or more widely separated OHCs (Fig. 4). Three (and occasionally 4) rows of OHCs were observed; innervated OHCs could be in the same or different rows. The tips of outer spiral fiber branches were generally marked by relatively small (less than 1 μm in diameter) and continuously convex swellings. Nine out of 87 terminal branches ended at the bases of OHCs without a visible terminal swelling. We do not know if these "free" endings are synaptic structures or artifacts due to fading of HRP reaction product, but we shall treat these nine as terminal branches. One outer spiral fiber bifurcated and gave rise to two spiralling, interweaving collaterals that terminated against adjacent OHCs. Outer spiral fiber characteristics for traced and untraced cells are summarized in Table 2.

Cell body characteristics

The cell bodies of type I and type II neurons were qualitatively similar with respect to size and shape (Fig. 5). Type I cell bodies (129.5 $\pm$ 5.0 μm^2) tended to be slightly larger

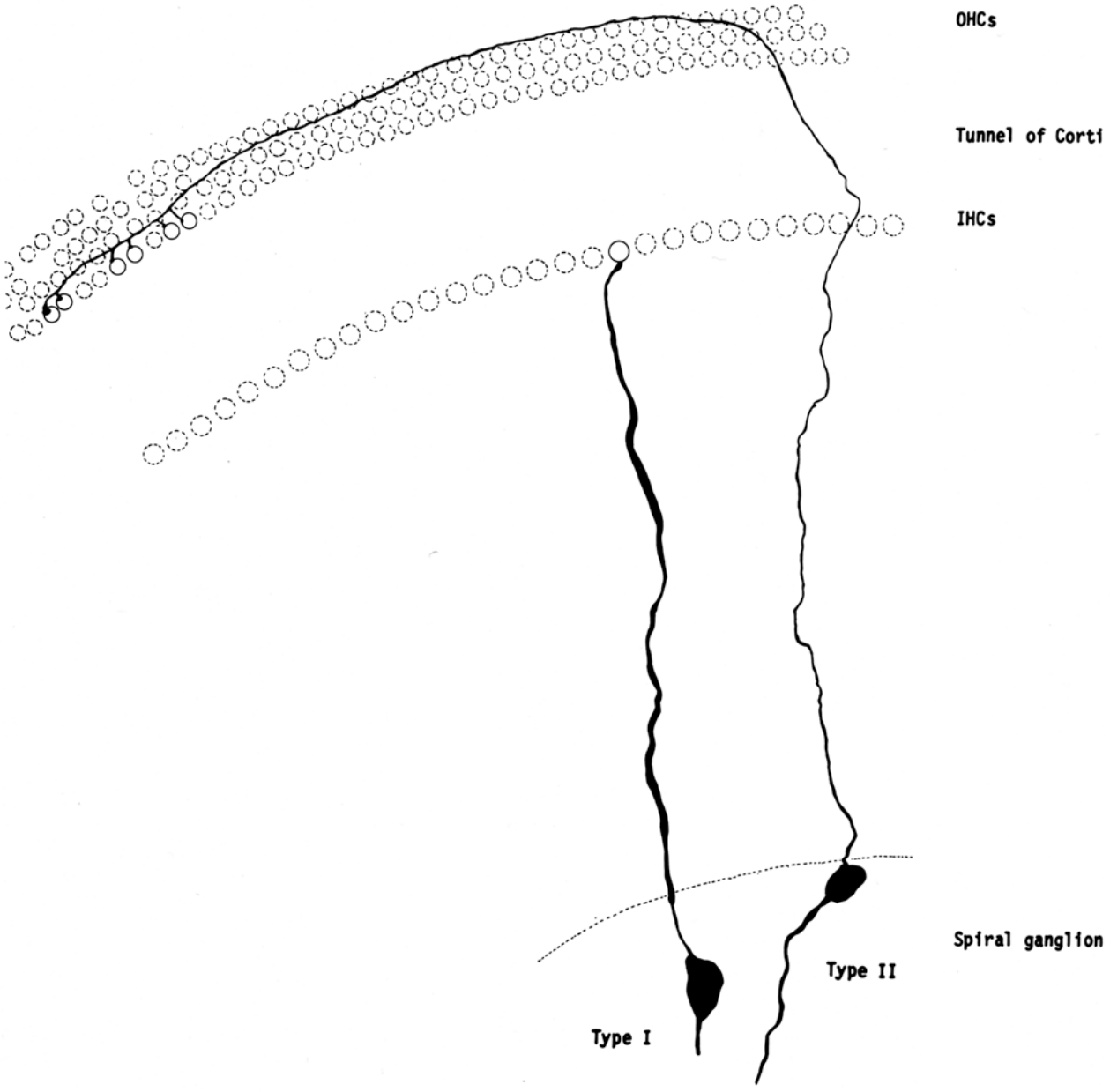

Fig. 2. Composite drawing tube reconstruction of HRP-labelled type I and type II neurons. These neurons are representative of the mouse cochlea. The type I neuron gives rise to a thin peripheral process that thickens as it courses across the osseous spiral lamina to terminate on a single IHC. The type II neuron sends a continuously thin process that crosses the tunnel of Corti, spirals basally, and then terminates on several OHCs. Scale bar equals 10 μm.

on average than those of type IIs (114.0 $\pm$ 5.7 μm^2) based on silhouette area ($P < .01$). Most type II cell bodies are less than 120 μm^2 in area, whereas most type I cell bodies are greater than 120 μm^2. Three of the type II cell bodies (from two animals) were distinctly larger than the other type II somata. No correspondence was found between type II cell body size and relative position in the spiral ganglion, peripheral process length, or number of terminal branches.

The somatic shape of both cell types appeared bipolar due to elongation in the plane of the diametrically opposed processes. This similarity in shape was represented by corresponding values for long/short axis ratios. In a few cases for both cell types, the two processes were positioned asymmetrically around the somata, and the cell body approached a pseudomonopolar shape.

The cell bodies of type I and type II neurons were not, however, uniformly distributed within the spiral ganglion. Along the length of the cochlear spiral, type I cell bodies were distributed all across the radial dimension of the ganglion, whereas type II cell bodies were located predominantly in the outer half of the ganglion (closest to the organ of Corti). This difference was quantified by measuring the radial distance from the geometric center of each cell body to the peripheral boundary of the ganglion as seen in the

TABLE 1. Summary of Spiral Ganglion Cell Characteristics

Features	Type I $\bar{x} \pm$ SEM	Type II $\bar{x} \pm$ SEM	P value
No. of neurons	n = 29	n = 13	
Peripheral innervation	IHCs	OHCs	
Cell-body area	129.5 ± 5.0 μm^2	114.0 ± 5.7 μm^2	<.01
Long/short axis ratio (somatic roundness)	1.8 ± 0.09	1.7 ± 0.14	NS
DC	1.1 ± 0.05 μm	1.0 ± 0.04 μm	NS
DP-1	0.5 ± 0.03 μm	0.9 ± 0.04 μm	<.001
DP-2	1.1 ± 0.05 μm	0.6 ± 0.03 μm	<.001
DP-3	1.4 ± 0.07 μm	0.4 ± 0.03 μm	<.001
DC/DP-1	2.5 ± 0.18	1.1 ± 0.04	<.001
DP-2/DP-1	2.4 ± 0.15	0.8 ± 0.04	<.001
DP-3/DP-1	3.0 ± 0.18	0.4 ± 0.04	<.001
Distance from cell body to periphery of spiral ganglion	74.9 ± 7.9 μm	33.0 ± 4.7 μm	<.01

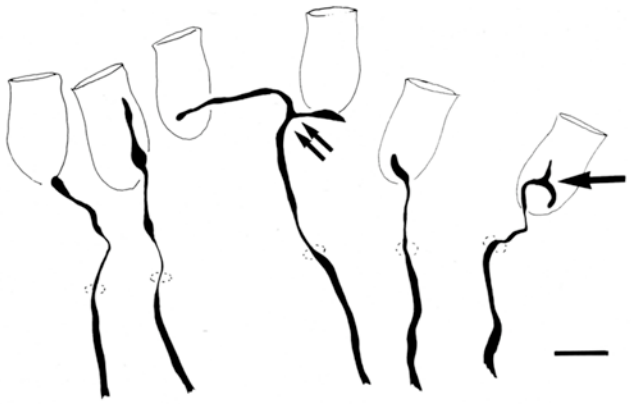

Fig. 3. Composite drawing tube reconstructions of radial fibers and their terminal endings. Each radial fiber is thin as it passes through a foramen nervosum (dotted rings). Most radial fibers were unbranched and terminated as a single swelling. Two radial fibers branched and terminated on one (arrow) or two (double arrow) hair cells. Terminal swellings contacted the body of IHCs, and ranged in size from 0.9 to 18.1 μm^2 (mean 5.16 ± 0.8 μm^2). Scale bar equals 10 μm.

histological section (range: 9–218 μm). The average distance for cell bodies of type II neurons was 33.0 ±4.7 mm, whereas that for type I neurons was 74.9 ± 7.9. μm.

Process characteristics

The average diameter of the central processes for the two ganglion cell types was similar (approximately 1 μm) when measured in the vicinity of the cell body. In contrast, the average diameter of peripheral process segments measured at three sites along the peripheral trajectory differed for the two neuron types (Table 1). These measurements revealed that during their course across the osseous spiral lamina, radial fibers increase in diameter, whereas outer spiral fibers gradually taper.

Morphological indicators

Although the direct tracing of neurons to their receptor cells is the most unambiguous method for identifying ganglion cell type, the procedures are technically demanding. In the present study, we sought morphological features that were more readily available and indicative of the two types of neurons. The most reliable (but not necessarily absolute) chracteristics that distinguished the two cell types were certain structural dimensions of the process in the vicinity of the cell body. For example, the peripheral processes (DP-1) of neurons giving rise to radial fibers were relatively thin compared to those giving rise to outer spiral fibers (Fig. 6A). Since the central processes of both types were similar in caliber, the ratio of central process diameter (DC) to peripheral process diameter (DP-1) was usually greater for neurons innervating IHCs than for neurons innervating OHCs (Fig. 6B). (The separation of data points representing the two cell types increased further when the ratio of peripheral process diameters (DP−2/DP−1) was used (Fig. 6C). The separation was maximal when DP−3/DP−1 was used, but we have not shown this relationship because measurements of DP−3 were only obtained from reconstructed fibers). When pooling traced and untraced data from eight animals, the groupings are obscured.

Distinctions between type I and type II neurons are more evident when analyses are conducted within a single animal (Fig. 7). For each animal, the segregation of data points into two clusters is indicative of the separate neuronal populations. Note how the relative positions of data points maintain this separation despite minor variations in absolute values along the abcissa. By this animal-by-animal analysis, therefore, the interpretation of pooled data (see Fig. 6D) is facilitated (Fig. 8).

DISCUSSION

The present results in adult mice indicate that acoustic receptors are innervated by two separate populations of spiral ganglion neurons: type I and type II neurons. Each type I neuron contacts only one or sometimes two IHCs, whereas each type II neuron contacts on average six OHCs. This segregation of pathways from the different acoustic receptors form two afferent systems that on the basis of morphological grounds should subserve different functions. Our observations are consistent with the hypothesis that the dual system of afferent organization may be a general feature of the mammalian cochlea (Kiang et al., '82, '84).

The segregation of hair cell afferents in adults as demonstrated with HRP techniques (Kiang et al., '82; present data), however, does not wholly agree with Golgi descriptions in neonatal mammals whereby single ganglion cells can innervate both IHCs and OHCs (e.g. von Ebner, '03, Fig. 1470; Lorente de Nó, '37, Fig. 1; Polyak et al., '46 Fig. 81). Such descriptions, especially in newborn mammals, show drawings of single ganglion cells that ramify around both receptor types. These various descriptions may all be accurate if it is postulated that single cell innervation of IHCs and OHCs represents an immature and transient pattern. There is some support for this notion from observations on tissue impregnated by Golgi methods; Perkins and Morest ('75) report that single fibers innervating both types of receptors were not observed in kittens older than 1 day of age.

Extensive branching of radial fibers has also been observed in immature mammals (Retzius, 1892; Ramón y Cajal, '09; Held, '26; Perkins and Morest, '75). Most fibers were found to branch multiple times and innervate at least

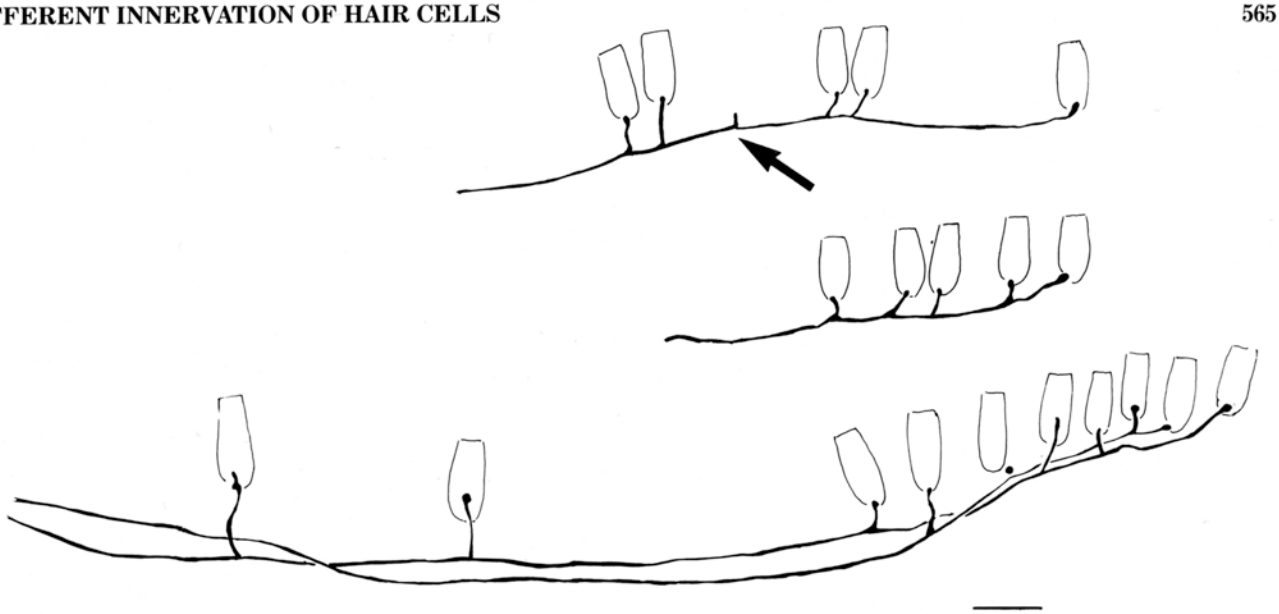

Fig. 4. Composite drawing tube reconstructions of outer spiral fibers and their terminal endings. Typically, outer spiral fibers exhibited a single process that terminated by sending short branches with bouton endings to several (three to ten) OHCs. One outer spiral fiber (bottom) bifurcated and gave rise to two collateral processes. In some instances, branches ended blindly without a terminal swelling (arrow). Scale bar equals 10 μm.

TABLE 2. Innervation Data for Reconstructed Outer Spiral Fibers in the Middle Third of the Cochlear Duct

Fiber	Bifurcated	Spiral length (μm)	Terminal spiral length (μm)	No. of terminal branches	Innervated row of OHCs
Traced to cell body					
4	No	269	76	8	1
5	No	450	272	6	3
6	Yes	416	256	6	2,3
	—	—	256	4	2,3
7	No	275	52	7	1
8	No	214	44	7	1,2
9	No	234	47	10	3
12	No	372	89	6	3
3	No	330	47	5	2,3
Untraced fibers					
1	No	426	124	9	3
2	No	254	51	3	3
3	No	470	45	5	2
4	No	399	60	4	2
5	No	361	75	3	1
6	No	355	60	4	1

two IHCs in young animals, whereas such branching was rarely found in adult animals (Liberman, '82; present data). There is a hint that outer spiral fibers are also more extensively branched in very young mice than in adult mice. In Figure 1 of Lorente de Nó ('37), there are three outer spiral fibers, each of which gives rise to roughly ten terminal branches and several additional varicosities; these are more than the six branches typically found in adults. We would hypothesize that the terminal arbors of both types of primary peripheral processes are progressively reduced during postnatal maturation. Following the maturational remodeling of the afferent arborization, there remain two types of peripheral processes: A simple, usually unbranched process (radial fiber) that gives rise to a single swelling and a spiraling, branched process (outer spiral fiber) that gives rise to multiple swellings. The notion that differences in afferent innervation exist between cochleas of mature and immature animals is not new (e.g. von Ebner, '03) and is consistent with current ideas that exuberant connections retract and the innervation field becomes limited as the animal develops (e.g., Innocenti et al., '77; Jackson and Parks, '82; Stanfield and O'Leary, '85; Whitehead and Morest, '85).

Descriptions of cell bodies of spiral ganglion neurons have been provided for a number of mammalian species (e.g. guinea pig, Thomsen, '66; cat, Spoendlin, '73; man, Ota and Kimura, '80; opossum, Kiang et al., '84; rat, Bichler, '84). Despite differences in species, ages of the animals studied, histological methods, and descriptive criteria, it is generally accepted that there are two types of neuronal cell bodies in the mammalian spiral ganglion: a majority group of neurons (type I) with large cell bodies composing 90–95% of the population and a minority group of neurons (type II) with small cell bodies composing the remaining 5–10%. The segregated innervation of hair cells by type I and type II neurons has now been demonstrated in cats (Kiang et al., '82), mice (present results), rats (unpublished observation), and guinea pigs (M.C. Brown, personal communication). These observations are consistent with the notion that the two hair cell systems have separate pathways into the brain.

The two populations of spiral ganglion neurons may also be distinguished by more accessible and quantifiable features visible with the light microscope. For example, process characteristics in the vicinity of the cell body have been shown to provide fairly reliable indicators for the type of receptor innervation. Specifically, peripheral processes of most ganglion cells exhibit a short but extremely thin segment that then abruptly expands (Kolmer, '27). These thin peripheral process segments are chracteristic of radial fibers innervating IHCs (Kiang et al., '82). In contrast, continuously thin peripheral processes are featured by outer

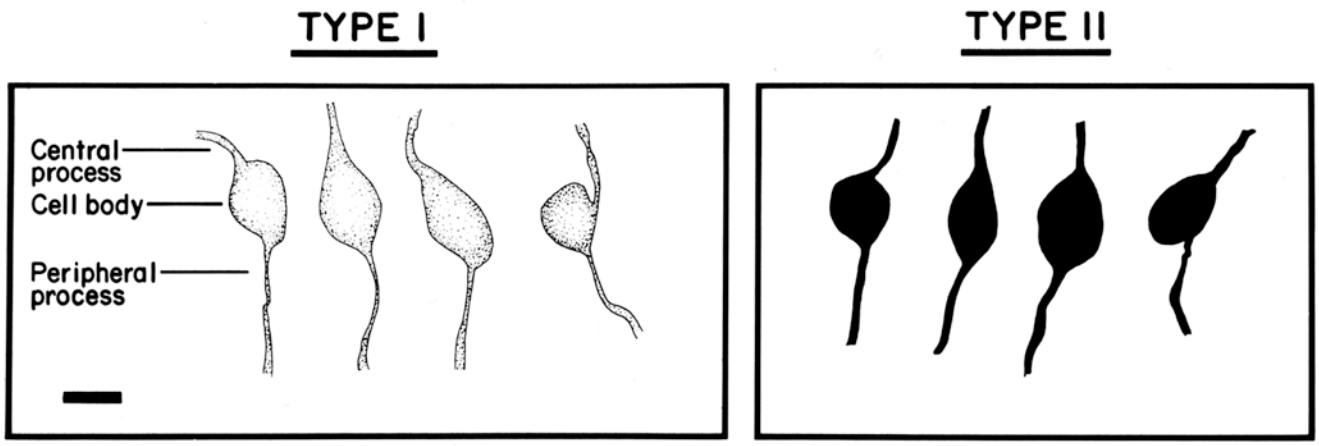

Fig. 5. Drawing tube reconstructions of cell bodies and initial processes of type I and type II neurons. This figure illustrates that the two types of ganglion cells cannot be readily distinguished on the basis of cell body shape or size. The thin peripheral process in the vicinity of the cell body, however, is indicative of type I neurons. Scale bar equals 10 μm.

spiral fibers innervating OHCs. These observations indicate that it should be possible to predict peripheral innervation in a sample of unreconstructed spiral ganglion neurons across different mammalian species. The practical significance is that ganglion cell identification can be made in cochlear tissue without reconstructing each peripheral process.

On the basis of a quantitative description of process characteristics, a general segregation of the spiral ganglion cell populations was found in the present sample of mice. The grouping of cell types became more striking with the use of ratios rather than actual measurements, presumably because ratios tend to reduce the problem of absolute size errors resulting from differential tissue shrinkage during histological processing or other sources of size variability (e.g., age, weight). The separation of cell types improved further by examining process chracteristics on an animal-by-animal basis. There is a definite "blurring" of boundaries when pooling data across animals. These observations emphasize that within-animal analyses may represent the most accurate method for interpreting the significance of measurements used in quantitative comparisons.

Type I neurons typically have larger cell bodies than do type II neurons (e.g., man, cat, rat). Ramón y Cajal ('09) reported that the size of a cell body was related to the diameter of its axis cylinder and to its arborization of collaterals and terminals. Thus, the smaller cell body of type II neurons might reflect reduced metabolic requirements for sustaining a more delicate central arborization of its axon. These observations are consistent with the notion that cytoplasmic volume is proportional to axonal and terminal volume.

What is perhaps curious is that certain other morphological distinctions (e.g., bipolar vs. pseudomonopolar or myelinated vs. unmyelinated) that helped to established this neural dichotomy are not consistent across species. Cell body shape of spiral ganglion neurons in cats has been described as either bipolar or pseudomonopolar (Kiang et al., '84). These two shapes have been operationally defined in that pseudomonopolarity occurs when the two processes emerge from the cell body without any visible convexity of the cell body between the two processes. In different mammals (e.g. man, cat, guinea pig, rat, mouse), large neurons (type I) tend to be bipolar. In contrast, small neurons (type II) can be bipolar (man, Ota, and Kimura, '80; guinea pig, Suzuki et al., '63; mouse, present results), pseudomonopolar (cat, Kiang et al., '82; guinea pig, Kiang et al., '84; man, Ota and Kimura '80), or multipolar (man, Ota and Kimura, '80; rat Ross and Burkel, '73). Finally, large type I neurons of cats have myelinated cell bodies and small type II neurons have unmyelinated cell bodies (Spoendlin, '73). In man, however, both types of spiral ganglion neurons tend to have unmyelinated cell bodies (Ota and Kimura, '80). At present, the role of cell body myelination and shape in auditory function is unknown.

Along these same lines, it has been of considerable interest to understand the significance of the variations in receptor innervation density, both as a function of receptor type, receptor position on the basilar membrane, and of individual species. Innervation density has been viewed in terms of the ratio of ganglion cells to receptor type or the ratio of afferent terminals to receptor type (Ramprashad et al., '78; Bruns and Schmieszek, '80). The two ratios are the same for type I neurons because radial fibers do not usually branch and give rise to only a single terminal. Although innervation density is known to vary from cochlear base to apex, an average number of type I primary afferent terminals per IHC can be determined on the basis of figures published in the literature. The number is eight for man (Guild et al., '31; Held, '26), ten for guinea pig (Firbas, '72), 13 for mouse (Ehret and Frankenreiter, '77; Ehret, '79; Keithley and Feldman, '83) and 20 for cat (Gacek and Rasmussen, '61; Spoendlin, '73). There is significantly less known about afferent innervation density for OHCs, an issue complicated by the amount of outer spiral branching (Smith, '75). The number of primary afferent terminals per outer hair cell (calculated by multiplying the number of type II cell bodies by the average number of terminals per outer spiral fiber and dividing by the number of OHCs) is roughly similar for mouse (two to three) and guinea pig (four to five). These values are also in the range of those determined by electron microscopic examination of OHCs. The number is three for horseshoe bat (Bruns and Schmieszek, '80) and four for cat (Spoendlin, '73). It seems that these fluctuations of innervation density across the above mentioned series of mammals represent relatively minor

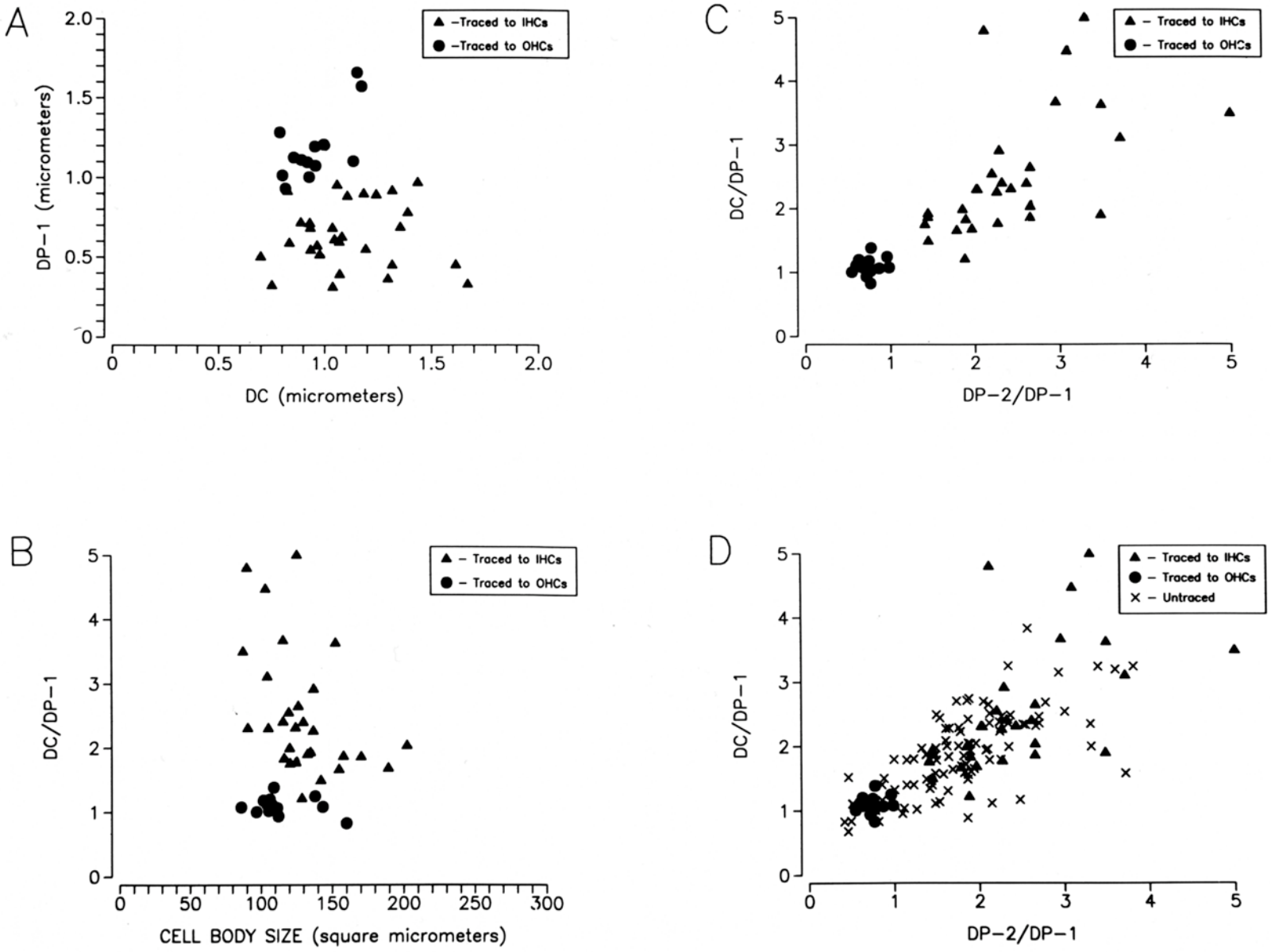

Fig. 6. Quantitative features that predict peripheral innervation. A. Central process diameter (DC) plotted against peripheral process diameter (DP-1). The peripheral process values for fibers traced to IHCs are consistently smaller than those for fibers traced to OHCs, but the central process values are overlapping. B. Process ratios (DC/DP-1) plotted against cell body area. C. DC/DP-1 ratios plotted against DP-2/DP-1 ratios for traced type I and type II neurons. D. DC/DP-1 ratios plotted against DP-2/DP-1 for traced and untraced neurons.

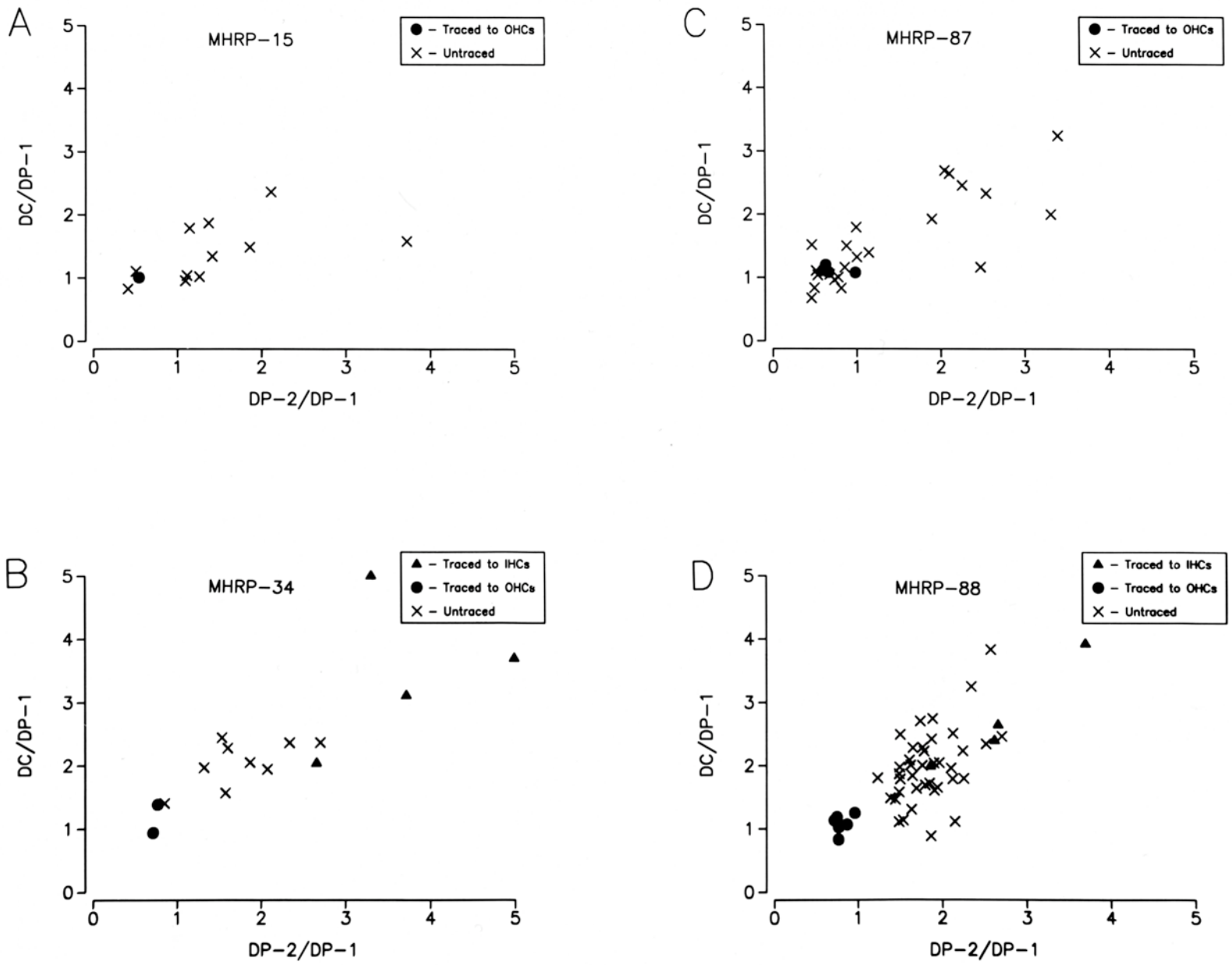

Fig. 7. Process ratios for individual animals. The data points fall into two clusters. An imaginary vertical line divides the two clusters of data points, but its value for individual animals varies from roughly 0.7 to 1.5.

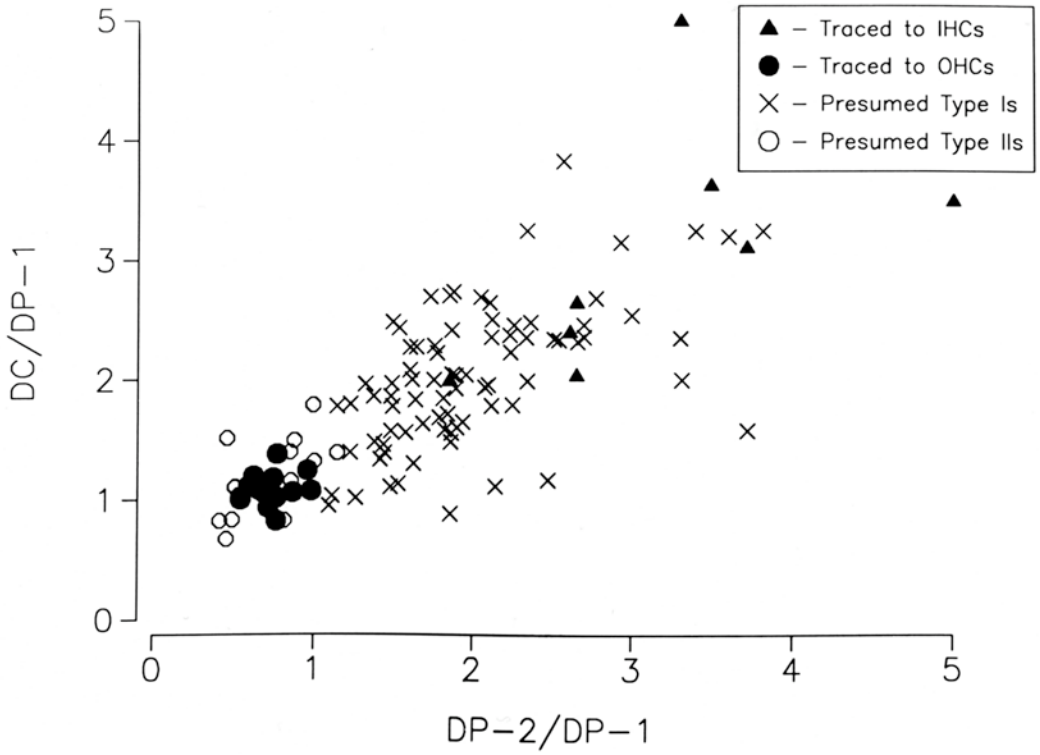

Fig. 8. Process ratios pooled across four animals. The animal-by-animal analysis from Fig. 7 was used to clarify the pooled data.

thematic variations and may not have any significant effect on auditory function. What then is the significance of the observation that in the little brown bat (*Myotis lucifugus*), but not in all echo-locating bats, there are three to seven times as many afferents per IHC (70, Ramprashad et al., '78) as in other mammals? Although we do not presently have the answers, by considering these structural variations in light of the acoustic requirements and behavioral adaptations of individual species, we may gain insight into the structural features that contribute to specific functions in the biology of hearing.

ACKNOWLEDGMENTS

The authors thank D.D. Simmons for contributions made during the initial stage of the project, S. Keene and R. Cronin-Schreiber for help with illustrations, P. Ley for photographic assistance, and R.G. Vega for typing assistance. The authors also thank T.E. Benson, M.C. Brown, M.C. Liberman, and M.R. Szpir for helpful comments on the manuscript. This research was supported by NIH grants NS13126, NS20156, and GMO7258 and by the Milton Foundation of Harvard Medical School. Some of these results were presented in preliminary form at the 15th annual meeting of the Society for Neuroscience, Dallas, TX 1985.

LITERATURE CITED

Bichler, E. (1984) Some morphological features of neurons in the rat spiral ganglion. Arch. Otorhinolaryngol. *240*:243–248.

Bock, G.R., and K.P. Steel (1984) Use of albino animals for auditory research. Hear. Res. *13*:201–202.

Bruns, V., and E. Schmieszek (1980) Cochlear innervation in the greater horseshoe bat: Demonstration of an acoustic fovea. Hear. Res. *3*:27–43.

Davis, H. (1958) Transmission and transduction in the cochlea. Laryngoscope *68*:359–382.

Ehret, G. (1979) Quantitative analysis of nerve fibre densities in the cochlea of the house mouse (*Mus musculus*). J. Comp. Neurol. *183*:73–88.

Ehret, G., and Frankenreiter (1977) Quantitative analysis of cochlear structures in the house mouse in relation to mechanisms of acoustical information processing. J. Comp. Physiol. *122*:65–85.

Firbas, W. (1972) Uber anatomische Anpassungen des Hörorgans an die Aufnahme hoher Frequenzen. Mschr. Ohr.hk. Laryngol.-Rhinol., Vienna *106*:105–156.

Frank, E., W.A. Harris, and M.B. Kennedy (1980) Lysophosphatidyl choline facilitates labeling of CNS projections with horseradish peroxidase. J. Neurosci. Methods *2*:183–187.

Gacek, R.R., and G.L. Rasmussen (1961) Fiber analysis of the statoacoustic nerve of guinea pig, cat and monkey. Anat. Rec. *139*:455–463.

Ginzberg, R.D., and D.K. Morest (1983) A study of cochlear innervation in the young cat with the Golgi method. Hear. Res. *10*:227–246.

Guild, S.R., S.J. Crowe, C.C. Bunch, and L.M. Polvogt (1931) Correlations of differences in the density of innervation of the organ of Corti with differences in the acuity of hearing, including evidence as to the location in the human cochlea of the receptors for certain tones. Acta Otolaryngol. (Stockh.)*15*:269–308.

Held, H. (1926) Die Cochlea der Säuger and der Vögel, ihre Entwicklung und ihr Bau. In: Handbuch der normalen and pathologischen Physiologie XI, Berlin: Springer pp.467–534.

Henry, K.R. (1983) Ageing and audition. In: J.F. Willot (ed): The Auditory Psychobiology of the Mouse. Springfield, IL: Charles C Thomas Publishers, pp. 470–493.

Innocenti, G.M., L. Fiore, and R. Caminiti (1977) Exuberant projection into the corpus callosum from the visual cortex of newborn cats. Neurosci. Lett. *4*:237–242.

Jackson, H., and T.N. Parks (1982) Functional synapse elimination in the developing avian cochlear nucleus with simultaneous reduction in cochlear nerve axon branching. J. Neurosci. *2*:1736–1743.

Keithley, E.M., and M.L. Feldman (1983) The spiral ganglion and hair cells of Bronx waltzer mice. Hear. Res. *12*:381–391.

Kiang, N.Y.–S., J.M. Rho, C.C. Northrup, M.C. Liberman, and D.K. Ryugo

(1982) Hair-cell innervation by spiral ganglion cells in adult cats. Science *217*:175–177.

Kiang, N.Y.–S., M.C. Liberman, J.S. Gage, C.C. Northrup, L.W. Dodds, and M.E. Oliver (1984) Afferent innervation of the mammalian cochlea. In L. Bolis, R.D. Keynes, and S.H.P. Maddrell (eds): Comparative Physiology of Sensory Systems. Cambridge: Cambridge University Press, pp. 143–161.

Kolmer, W. (1927) Gehörorgan. In: Handbuch der mikroskopischen Anatomie des Menschen. Band III. Berlin: Springer Verlag, pp. 351–367.

Liberman, M.C. (1982) The cochlear frequency map for the cat: Labeling auditory-nerve fibers of known characteristic frequency. J. Acoust. Soc. Am. *72*:1441–1449.

Liberman, M.C., and M.E. Oliver (1984) Morphometry of intracellularly labelled neurons of the auditory-nerve: correlations with functional properties. J. Comp. Neurol. *223*:163–176.

Lorente de Nó, R. (1937) Neural mechanism of hearing. I. Anatomy and physiology (b) Sensory endings in the cochlea. Laryngoscope *47*:373–377.

Münzer, F.T. (1931) Uber markhaltige Ganglienzellen. Z. Mikrosk. Anat. Forsch. *24*:286–361.

Ota, C.Y., and R.S. Kimura (1980) Ultrastructural study of the human spiral ganglion. Acta Otolaryngol. (Stockh.) *89*:53–62.

Perkins, R.E., and D.K. Morest (1975) A study of cochlear innervation patterns in cats and rats with Golgi method and Nomarski optics. J. Comp. Neurol. *163*:129–158.

Polyak, S.L., G. McHugh, and D.K. Judd (1946) The Human Ear in Anatomical Transparencies. Elmsford, NY: Sonotone.

Ramón y Cajal, S. (1909) Histologie du Système Nerveux de l'Homme et des Vertébrés, Vol. I. (1952 reprint). Madrid, Spain: Instituto Ramón y Cajal.

Ramprashad, F., K.E. Money, J.P. Landolt, and J. Laufer (1978) A neuroanatomical study of the cochlea of the little brown bat (*Myotis lucifugus*). J. Comp. Neurol. *178*:347–364.

Rasmussen, A.T. (1943) Outlines of Neuroanatomy. Dubuque, IA: Brown.

Retzius, G. (1892) Die Endigungsweise des Gehörnerven. Biolog. Untersuchungen, Neue Folge, III. Leipzig: Vogel.

Ross, M.D., and W. Burkel (1973) Multipolar neurons in the spiral ganglion of the rat. Acta Otolaryngol. (Stockh.) *76*:381–394.

Ryugo, D.K., and F.H. Willard (1985) The dorsal cochlear nucleus of the mouse: A light microscopic analysis of neurons that project to the inferior colliculus. J. Comp. Neurol. *242*:381–396.

Smith, C.A. (1975) Innervation of the cochlea of the guinea pig by use of the Golgi stain. Ann. Otolaryngol. *84*:443–458.

Spoendlin, H. (1973) The innervation of the cochlear receptor. In A.R.Møller (ed): Basic Mechanisms in Hearing. New York: Academic Press, pp. 185–234.

Stanfield, B.B., and D.D.M. O'Leary (1985) The transient corticospinal projection from the occipital cortex during the postnatal development of the rat. J. Comp. Neurol. *238*:236–248.

Suzuki, Y., A. Watanabe, and M. Osada. (1963) Cytological and electron microscopic studies on the spiral ganglion cells of adult guinea pigs and rabbits. Arch. Histol. Jpn. *24*:9–33.

Thomsen, E. (1966) Ultrastructure of the spiral ganglion in the guinea pig. Acta Otolaryngol. [Suppl.] (Stockh.) *224*:442–448.

Von Ebner, B. (1903) Die Endigung des Schneckennerven im Cortischen Organe. Kölliker's Handbuch der Gewebelehre des Menschen, III. Leipzig: Engelmann, pp. 944–960.

Weiss, T.F. (1984) Relation of receptor potentials of cochlear hair cells to spike discharges of cochlear neurons. Annu. Rev. Physiol. *46*:247–259.

Whitehead, M.C., and D.K. Morest (1985) The development of innervation patterns in the avian cochlea. Neuroscience *14*:255–276.